Nature Environment and Pollution Technology
An International Quarterly Scientific Journal

p-ISSN: 0972-6268
(Print copies up to 2016)
e-ISSN: 2395-3454

Vol. 25 | No. 3 | Article ID B4409 | 2026

Original Research Paper

https://doi.org/10.46488/NEPT.2026.v25i03.B4409

Open Access Journal

Black Gold from the Fields: Obtaining Pyrolytic Biochar from Agricultural Wastes at Various Pyrolysis Temperatures

Pooja Sarolkar, Girish Pathade and Wasim Bagwan
Krishna Institute of Science and Technology, Krishna Vishwa Vidyapeeth (Deemed to be University), Karad, 415539, Maharashtra, India
†Corresponding author: Pooja S. Sarolkar; sarolkarpuja07@gmail.com

Abbreviation: Nat. Env. & Poll. Technol.
Website: www.neptjournal.com

Received: 23-10-2025
Revised: 10-12-2025
Accepted: 15-12-2025

Key Words:

Biochar
Pyrolysis
Finger millet hulls
Agricultural residue
Soil amendment
Carbon sequestration

Citation for the Paper:

Sarolkar, P., Pathade, G. and Bagwan, W., 2026. Black gold from the fields: Obtaining pyrolytic biochar from agricultural wastes at various pyrolysis temperatures. *Nature Environment and Pollution Technology*, 25(3), B4409. https://doi.org/10.46488/NEPT.2026.v25i03.B4409

Note: From 2025, the journal has adopted the use of Article IDs in citations instead of traditional consecutive page numbers. Each article is now given individual page ranges starting from page 1.

ABSTRACT

India produces a large amount of agricultural residues, traditionally disposed of through open burning. Such practices have negative health and environmental impacts. Converting waste via pyrolysis into biochar offers a sustainable strategy for enhancing soil fertility, carbon sequestration, and resource recovery. Although many studies have examined the influence of pyrolysis temperature on biochar properties, most focus on feedstocks like rice husk and woody biomass, with little attention given to underused residues such as finger millet husk. This study evaluated four agricultural residues, finger millet husk, rice husk, sawdust, and hardwood, depolymerized at 300, 400, 500, and 600°C, respectively. The resulting biochars underwent proximate and ultimate analysis, physicochemical characterization, and assessments of pore size and surface morphology. Results showed that increasing pyrolysis temperature reduced biochar yield and volatile matter, while increasing fixed carbon, pH, organic carbon content, porosity, and surface area. Variations also depended on feedstock composition. Biochar from finger millet husk at 300°C was flaky, chemically active, and suitable for microbial colonization, whereas hardwood biochar at 600°C was highly carbonized, porous, stable, and effective for pollutant adsorption and long-term carbon sequestration. This research introduces finger millet husk as a novel biochar precursor, linking specific properties to potential agricultural and environmental applications. Additionally, the study emphasizes how pyrolysis temperature influences biochar characteristics and their practical uses.

1. INTRODUCTION

As a developing country, India relies heavily on agriculture, which employs approximately 70% of the population (Mathur & Srivastava 2019). Annually, agricultural activities produce around 500 million tons of waste residues (Nagar & Kumar 2024). Typically, Indian farmers manage this biomass through traditional methods, mainly open-field burning, which worsens air quality and poses health risks. Recent studies have shown that these burning practices significantly impact population dynamics, meteorological stability, and environmental conditions from 2003 to 2019 (Lan et al. 2022). Additionally, between 2011 and 2020, biomass burning contributed to about 75% of atmospheric pollution in India, causing periodic spikes in suspended particulate matter (PM10 and PM2.5) and leading to serious respiratory and cardiovascular health problems (Gupta 2019).

In contrast, a renewable carbonaceous biochar derived from waste biomass through pyrolysis serves as an environmentally friendly substitute. The pyrolysis process reduces pollutant emissions and produces bioenergy that can replace non-renewable energy sources (Chatterjee et al. 2020, Nadarajah et al. 2024). Biochar, a stable carbon-rich material created by pyrolysis, is commonly used as a soil amendment to improve soil fertility (Amalina et al. 2022). Numerous studies have explored its applications, including reducing greenhouse gas emissions, enhancing soil fertility, stimulating microbial growth, and functioning as an adsorbent for removing pollutants from wastewater (Abrishamkesh et al. 2015, Awasthi et al. 2020, Ge et al. 2019, Hossain et al. 2020, Muzyka et al. 2023, Wang et al. 2020). Biochar shows particular promise for specific biomass applications. For example, biochar from finger millet has been reported to lower pesticide soil toxicity and restore biological health (Jena et al. 2025). Rice husk biochar increases soil enzyme activity and beneficial microorganism populations such as *Massilia*, *Bacillus*, and *Trichocladium*, while also reducing loamy soil erosion in semi-arid areas (Akumuntu et al. 2024, Ahmadi et al. 2020). Similarly, sawdust biochar has a high adsorption capacity, which can be used to remove cadmium and lead from wastewater (Cheng et al. 2021), and it also shows potential for purifying industrial effluents contaminated with cyanide and other toxic metals (Manyuchi et al. 2022).

The efficacy of biochar and its physicochemical properties largely depend on production conditions, including the type of biomass and its composition, pyrolysis temperature, heating rate, and residence time (Mukherjee et al. 2022). For instance, increasing the pyrolysis temperature results in higher pH, ash content, and surface area, while reducing yield and O/C ratio (Roshan et al. 2023). Consequently, biochar produced at lower pyrolysis temperatures may offer a balance between energy efficiency and productivity enhancement, especially when using tropical agricultural by-products for carbon sequestration (Song et al. 2023). In this context, biochar derived from various biomass sources-such as forestry hardwoods, industrial sawdust, and agricultural wastes like rice husk and finger millet hulls-should be thoroughly studied for surface morphology, mineral composition, thermal behavior, heavy metal content, and both proximate and ultimate analyses. This paper aims to characterize and compare biochar from these feedstocks for its potential as a soil amendment and for carbon sequestration efforts.

2. MATERIALS AND METHODS

2.1. Collecting the Agricultural Residues and Production of Biochar

All agricultural wastes, including finger millet hull, sawdust, rice husk, and hardwood, were collected from farms and air-dried in the shade for 15 days. They were then cut into 2-3 cm pieces and stored in airtight zip-lock bags to reduce moisture. The experiments took place at Krishna Institute of Science and Technology, Krishna Vishva Vidyapeeth, Karad, Maharashtra, from January to April 2025. Biochar was produced from selected agro-wastes, specifically rice husk, sawdust, finger millet hull, and hardwood. These residues were thermally converted in a muffle furnace. Before pyrolysis, all biomass samples were oven-dried at 105°C for 24 h. A known weight of biomass was placed in a ceramic crucible with a tight-fitting cover and then transferred to the muffle furnace, where pyrolysis was carried out at temperatures of 300°C, 400°C, 500°C, and 600°C. The heating rate was maintained at 10°C per minute, with a residence time of 30 minutes at each temperature. After pyrolysis, the biomass was ground using a suitable grinder. The ground biochar was then sieved through a 150-micrometer mesh and stored in an airtight glass bottle to prevent moisture uptake and contamination.

2.2. Biochar Characterizations

2.2.1. Biochar Yield

The biochar yield, defined as the mass of pyrolysis products relative to the initial mass of raw material, was calculated using Eq. 1 from Khater et al. (2024) and Qin et al. (2020).

$$\text{Biochar yield (\%)} = \frac{\text{Weight of biochar after pyrolysis (g)}}{\text{Weight of feedstock before pyrolysis (g)}} \times 100 \quad ...(1)$$

2.2.2. Physical, Chemical, and Proximate Analysis of Biochar

The composition was mechanically shaken for one hour at 25°C, followed by a 30-min standing period. The pH and electrical conductivity (EC) of each biochar sample were then measured using pH and EC meters, with a biochar to distilled water ratio of 1:10 (Singh et al. 2017). To determine water holding capacity (WHC), distilled water and a 1:40 (w/v) biochar mixture were shaken for three days at 25°C, dried for twelve h at 105°C, and the WHC% was calculated using Equation (2) (Zhang et al. 2024). Organic carbon content in biochar was analyzed using the Walkley and Black (1934) method, as described by Rabbani et al. (2020). Additionally, estimates for N, P, K, Ca, and Mg were obtained following AOAC (2003).

Water Holding Capacity

$$\text{Water Holding Capacity (\%)} = \frac{(m_{sb} - m_{fp} - m_{bc})}{m_{bc}} \times 100 \quad ...(2)$$

Where:

- m_{sb} = mass of the water-soaked biochar with filter paper
- m_{fp} = mass of water-soaked filter paper
- m_{bc} = mass of dried biochar

The inherent moisture, volatile matter, ash, and fixed carbon content of biochar were measured using equations 3, 4, 5, and 6, respectively, following ASTM-1762-82 standards (Dhar et al. 2020). The moisture content was determined by drying the biochar at 105°C for 2 h, and the percentage of inherent moisture was calculated accordingly.

Inherent Moisture Content

$$\text{Inherent Moisture (wt.\%)} = \frac{W_{ad} - W_{105}}{W_{ad}} \times 100 \quad ...(3)$$

Where:

- W_{ad} = weight of air-dried biochar sample
- W_{105} = weight of biochar sample dried at 105°C for 2 h

1 g air-dried biochar sample (preheated at 105°C for 2 h) was heated at 950°C for 6 min in a furnace, and the percentage of volatile matter was calculated as follows,

Volatile Matter Content

$$\text{Volatile Matter (wt.\%)} = \frac{W_{105} - W_{950}}{W_{ad}} \times 100 \quad ...(4)$$

Where:

- W_{105} = weight of biochar sample dried at
- W_{950} = weight of biochar sample after heating at for 6 minutes
- W_{ad} = weight of air-dried biochar sample

A 1-g air-dried mass of 105°C was heated at the muffle furnace at 750°C for 6 h to determine (wt.%) ash content as follows:

Ash Content

$$\text{Ash (wt.\%)} = \frac{W_{105} - W_{750}}{W_{ad}} \times 100 \quad ...(5)$$

Where:

- W_{105} = weight of biochar sample dried at
- W_{750} = weight of biochar sample after heating at for 6 h
- W_{ad} = weight of air-dried biochar sample

Fixed carbon was calculated on a dry basis and estimated as follows:

Fixed Carbon Content

Fixed Carbon (wt.%) = 100 – [Ash (wt.%) + Volatile Matter (wt.%)] …(6)

2.2.3. Elemental Analysis

The elemental composition (C, H, N, S) of four biochar samples was determined using an elemental analyzer (JEOL JSM-IT200, YCIS Satara).

2.2.4. Brunauer-Emmett-Teller (BET), Scanning Electron Microscopy (SEM), and Surface Functional Groups

The specific surface areas of the activated carbons (ACs) were measured using an Autosorb1C instrument (Quantachrome, Japan). The specific surface area (SSA), BJH pore volume, and pore size distributions were derived from nitrogen adsorption/desorption isotherms using a Multipoint BET (Brunauer-Emmett-Teller) method, conducted with equipment obtained from the Physics Department of Shivaji University, Kolhapur. Surface morphology of the biochar was examined using SEM (YCIS, Satara). The surface functional groups present on the biochar samples were identified through Fourier transform infrared spectroscopy (FTIR) at Krishna Institute of Pharmacy, KVV, Karad. Prior to analysis, all samples were washed with deionized water to remove impurities, neutralized, dried at 105°C, and stored in airtight glass vials. Further sample preparation was carried out as per the requirements of specific analysis tests.

2.3. Statistical Analysis

Each experiment was conducted in triplicate, with results expressed as the mean ± SD. Pyrolysis temperature and biomass feedstock type influence biochar yield and properties (Excel 2021). Two-way ANOVAs were performed, followed by pairwise comparisons using Tukey's HSD test at a 95% confidence level ($p < 0.05$). One-way ANOVA analyses were applied within temperature treatments for each feedstock. The relationships between pyrolysis temperature and key biochar parameters were assessed using Pearson's.

3. RESULTS

3.1. Physicochemical Properties

3.1.1. Physical Properties

Table 1 presents the physical properties-namely moisture content, water holding capacity (WHC), and porosity-of biochar derived from finger millet hull, sawdust, rice husk, and hardwoods, produced at various pyrolysis temperatures (300°C, 400°C, 500°C, and 600°C). The data show that moisture content decreases as pyrolysis temperature increases. Specifically, moisture content reduced from 4.8%, 4.2%, and 2.8% to 2.5% for rice husk, sawdust, finger millet hulls, and hardwoods, respectively, across the temperature range. Biochar produced from finger millet hulls at 300°C exhibited the highest moisture content (4.8%), while hardwood-derived biochar at 600°C showed the lowest (2.8%). This trend indicates that higher pyrolysis temperatures promote water removal, likely because increased temperatures enhance water extraction efficiency and make the biochar more stable and hydrophobic (Sathyabama et al. 2025). However, lower pyrolysis temperatures may retain more volatile substances, potentially affecting pore structure and WHC. Consequently,

Table 1: Physicochemical properties of different biochar types at different temperature ranges.

Properties	Biochar type			
	FMB	SDB	RHB	HWB
Moisture content [%]	4.8	2.5	4.2	2.8
Water Holding Capacity [%]	62	75	86	94
pH	6.1	7.2	7.7	8.2
Organic carbon [%]	20	32.86	26.31	66.22
N [%]	0.3	1.4	1.44	0.64
P [%]	0.01	0.013	0.012	0.015
K [%]	0.3	0.31	0.33	0.37
C: N	66.7:1	2.04:1	4.4:1	3.8:1
Ca [per 100 g]	10	51	45.5	53
Mg [Mequ]	6.3	8.5	8.8	11.2
Ca:Mg	1.18:1	8:1	3:1	6.2

Note: Finger millet hull biochar (FMB), sawdust biochar (SDB), rice husk biochar (RHB), and hardwood biochar (HWB)

an increase in pyrolysis temperature positively influences biochar WHC, as observed in studies showing WHC for finger millet hull, sawdust, rice husk, and hardwoods rising from 62% to 94%, suggesting initially low WHC that improves with higher temperatures (Ulusal et al. 2021).

3.1.2. Chemical Properties

The chemical structure of biochar varies depending on the feedstock and pyrolysis temperature. Table 1 presents the analyzed chemical properties of different biochar types (FMB, RHB, and HWB) produced at 300, 400, 500, and 600°C, including pH, electrical conductivity (EC), organic carbon content, total NPK, and calcium/magnesium levels. Higher pyrolysis temperatures increase the hydrogen potential of biochar by reducing functional groups (-COOH and -OH) at elevated temperatures, resulting in naturally alkaline biochar suitable for neutralizing acidic soils (Ahmed et al. 2024, Chellappan et al. 2018, El-Naggar et al. 2019, Roshan et al. 2023). At a lower pyrolysis temperature of 300°C, FMB exhibits a pH of 6.1, whereas HWB becomes alkaline with a pH of 8.2 at 600°C. Biochar serves as a superior liming material compared to conventional lime due to its content of base metals, (bi)carbonates, surface organic functional groups (OFGs), and soluble organic compounds, all of which help neutralize soil acidity through calcareous effects, cation exchange, and precipitation reactions (Liu et al. 2025). Conversely, the acidic active sites of biochar in saline soils can enhance plant growth and improve soil quality (Soothar et al. 2021). This suggests that soil salinity may decrease biochar acidity, and vice versa. Sovova et al. (2024) observed that the partially alkaline nature of biochar, along with its satisfactory internal porosity, could potentially enrich both acidic and partially acidic soils.

The results further indicate that organic carbon (OC) production is also influenced by pyrolysis temperature. Hardwood charred at 600°C exhibited the highest OC content (66.22%), while finger millet hulls showed the lowest OC content (20%) at a pyrolysis temperature of 300°C. This suggests that, regardless of feedstock type, higher temperatures promote carbon enrichment in the biochar matrix. Elevated levels of OC and fixed carbon (FC) contribute to increased soil organic carbon (SOC), which persists over time, inhibiting carbon mineralization and enhancing carbon sequestration potential (Bo et al. 2023). Consequently, increasing pyrolysis temperature enhances biochar's carbon content, creating a more durable medium for long-term carbon sequestration.

The maximum nitrogen content of 1.44% was recorded in rice husk biochar produced at a pyrolysis temperature of 500°C, while the lowest nitrogen content of 0.3% was found in finger millet hull biochar at 300°C. Results showed that phosphorus (P) and potassium (K) contents increased significantly with higher pyrolysis temperatures. The highest P (0.015%) and K (0.37%) contents were observed in hardwood biochar at 600°C, whereas the minimum P (0.01%) and K (0.3%) contents were in finger millet hull biochar at 300°C. Additionally, increasing the pyrolysis temperature from 300°C to 600°C led to rises in calcium (Ca) and magnesium (Mg) contents: Ca increased from 10 to 53, and Mg from 6.3 to 11 μmol per gram, following the order finger millet hull < sawdust < rice husk < hardwood biochar. These findings align with those reported by Khater et al., who observed that increasing the pyrolysis temperature from 400 to 800°C enhances P, K, Mg, and Ca contents in biochar (Khater et al. 2024).

3.2. Surface Area and Porosity

The surface area and porosity of biochar are influenced by the pyrolysis temperature. An increase in pyrolysis temperature causes the breakdown of organic matter, which enhances the biochar's surface area and porosity (Tomczyk et al. 2020). However, beyond certain temperature ranges, there is a formation of additional micropores, which can reduce overall porosity. This reduction may be due to the rising ash content at higher temperatures, as the ashes can fill the pore spaces (Feng et al. 2020, He et al. 2024, Ippolito et al. 2020, Khater et al. 2024). Additionally, porosity and surface area depend on the biomass type. As shown in Table 2, sawdust biochar produced at 400°C exhibits the highest porosity (13.38%) and surface area (30.45 $m^2.g^{-1}$), while rice husk biochar, produced at 500°C, shows the lowest values with porosity at 3.20% and surface area at 6.403 $m^2.g^{-1}$. Higher porosity and larger surface area improve absorption capacity, making biochar more effective at removing pollutants (Wyatalska et al. 2023).

3.3. Proximate Analysis and Yield of Biochar

Fig. 1 illustrates the differences in the content of volatile matter, ash, and fixed carbon at various pyrolysis temperatures (300-600°C) for different feedstocks, including finger millet hull, sawdust, rice husk, and hardwoods. Additionally, the biochar yield decreased from 74% to 26% as the pyrolysis temperature increased from 300°C to 600°C, influenced by factors such as the varying ratios of lignin and cellulose content. The formation of ash at high temperatures indicates increased stability of the carbon percentage in biochar (Khater et al. 2024). As shown in Fig. 1, the biochar yield for hardwoods, rice husk, sawdust, and finger millet hull was 37.1%, 31.5%, 29.8%, and 27.8%, respectively. Hardwood biochar (HWB) had the highest fixed carbon content, reaching 76.54% at 600°C, while the finger millet hull (FMB), sawdust (SDB), and rice husk (RHB) contained 51.61%, 55.39%, and 69.15%, respectively. This suggests that biochar produced at higher pyrolysis temperatures contains more fixed carbon (Toczydlowski et al. 2023). Due to its relatively high carbon content, biochar is a versatile resource with potential applications including use in chemical synthesis, activated carbon production, and as a soil conditioner (Ahmed et al. 2024).

The ash content of biochar increases at higher production temperatures compared to lower temperatures. Specifically,

Table 2: Porosity and specific surface area of different biochar types at different temperature ranges.

Biochar Sample	Specific surface area [Multi-Point BET] $m^2.g^{-1}$	Total pore volume [$cc.g^{-1}$]	Porosity [%]	Avg. pore radius [Å]	Radius [nm]	Avg. pore diameter [nm]
Finger millet	28.01	0.02496	9.74	1.782e+01 Å (17.82 Å)	1.782 nm	3.564 nm
Saw dust	21.857	0.02076	8.10	1.900e+01 Å (19.00 Å)	1.900 nm	3.800 nm
Rice husk	30.45	0.03430	13.38	2.253e+01 Å (22.53 Å)	2.253 nm	4.506 nm
Hard wood	6.403	0.008206	3.20	1.829e+01 Å (18.29 Å)	1.829 nm	3.658 nm

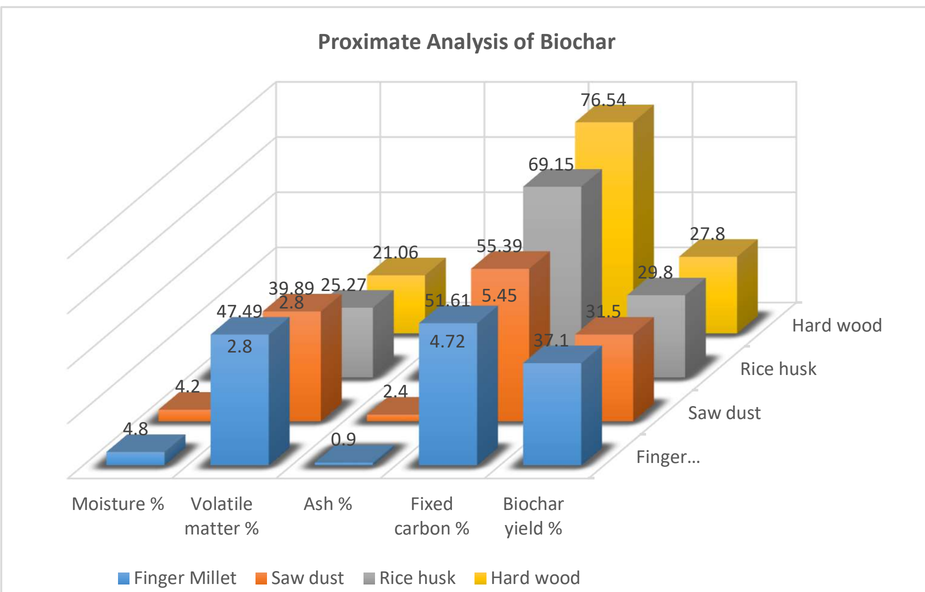

Fig. 1: Proximate analysis and yield of biochar types at different temperatures.

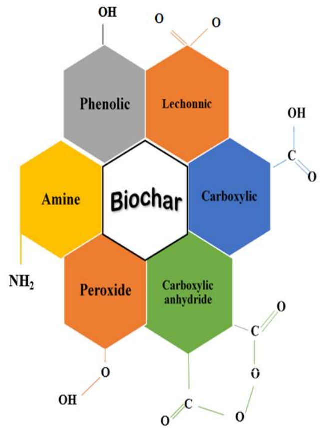

Fig. 2: Biochar containing surface functional groups.

the ash contents at 300, 400, 500, and 600°C are 0.9%, 2.4%, 4.72%, and 5.45%, respectively, for FMB, SDB, RHB, and HWB. Additionally, volatile matter tends to decrease as temperature rises. For example, FMB has a higher volatile content (47.49%) at 300°C than HWB, which has a lower volatile matter content (21.06%) at 600°C.

3.4. Surface Functional Groups

Biochar exhibits a range of functional groups on its surface, including hydroxyl (–OH), carboxyl (–COOH), lactonic (O–C=O), phenolic (–C=O), as well as peroxide and amine groups 22,23 (Fig. 2). These surface functional groups, particularly

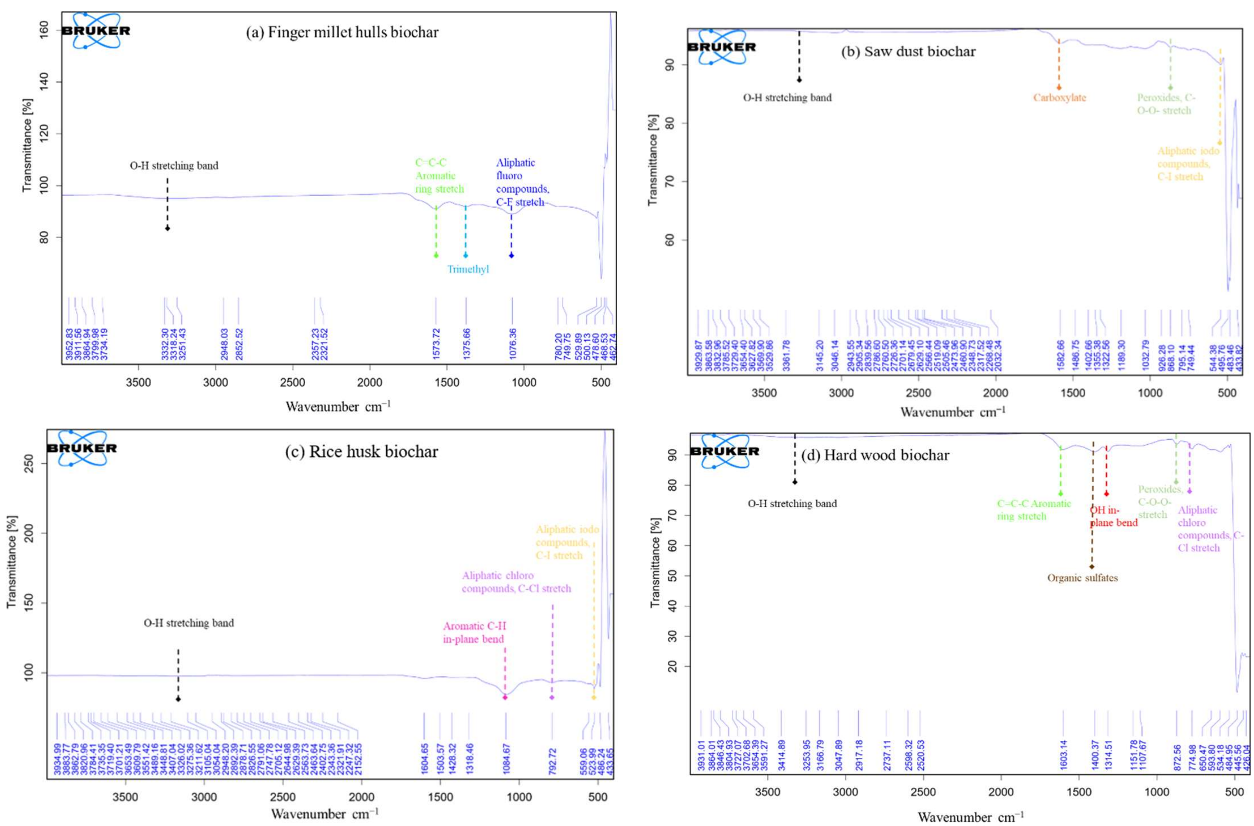

Fig. 3: FTIR spectra of biochar produced from (a) Finger millet, (b) Rice husk, (c) Sawdust, and (d) Hardwood.

C–O, C═O, and –OH, play a crucial role in contaminant decontamination and adsorption processes (Zhang et al. 2021). The structure of these groups is influenced by the molecular makeup of the biomass precursors and is largely determined by the pyrolysis temperature. For instance, cellulose and lignin primarily retain their structural features at 200–300°C, whereas biochar begins to lose most oxygen- and hydrogen-containing functional groups and becomes more aromatic at 500°C. Nevertheless, some functional groups, such as C=O in ketones and olefins, can survive even at 650°C (Zhang et al. 2020).

The surface functional groups and their quantification in numbers were determined using reference data from Coates (2000) and Nandiyanto et al. (2019). Fig. 3 illustrates variations in peak intensity, which occur because the concentration of specific functional groups is not uniform across samples [(a), (b), (c), and (d)]. The adsorption bands between 3360 and 3145 cm^{-1} confirm O-H stretching associated with hydroxyl groups. An increase in pyrolysis temperature reduces moisture retention, significantly influencing higher hydroxyl content, while weak aromatic C=C peaks indicate progressive thermal degradation or aromatization during biochar formation.

Peaks near 2940-2850 cm^{-1} correspond to C-H stretching vibrations of aliphatic $–CH_3$ and $–CH_2–$ groups, characteristic of cellulose and hemicellulose, observed in all four biochar samples [(a), (b), (c), and (d) Fig. 3] (Mujtaba et al. 2021). Additional functional groups identified include C=C–C aromatic ring stretching at 1615–1580 cm^{-1}, C–Cl stretching at 800-700 cm^{-1}, C–I stretching within 600-500 cm^{-1}, and C–F stretching between 1150 and 1000 cm^{-1}. The presence of trimethyl or tert-butyl groups was noted in the 1395–1385 cm^{-1} region. Other significant absorptions involved carboxylate groups (1610–1550 cm^{-1}), peroxides (C–O–O) at 890–820 cm^{-1}, organic sulfates at 1420–1370 cm^{-1}, and O-H in-plane bending at 1350-1260 cm^{-1}.

Collectively, these results demonstrate that pyrolysis conditions, biomass type, sample thickness, and particle size markedly influence the diversity and stability of surface functional groups on biochar, ultimately governing its chemical reactivity and environmental applications. The degree of carbonization notably affects biochar's surface functional morphology: highly carbonized biochar absorbs more IR radiation, decreasing transmittance and producing flatter or less intense peaks. Conversely, less carbonized or oxygen-rich samples exhibit higher transmittance and more prominent, distinct bands. Variations in mineral or ash content (e.g., silica in rice husk, carbonates in sawdust) further impact band intensity and sharpness due to their unique vibrational signatures.

3.5. Surface Morphology and Elemental Analysis

Fig. 4 depicts the surface morphology of biochar derived from four different agricultural waste materials: Finger Millet, Rice Husk, Sawdust, and Hardwood. All images were captured at 1500× magnification with a scale bar of 50 μm. The biochar made from finger millet hull at 300°C (a) exhibits irregular, flaky particles with a layered fractured surface, high porosity, and a rough texture, which are advantageous for adsorption applications and microbial colonization (Varkolu et al. 2025). The rice husk biochar produced at 400°C (b) appears dense with a grainy structure, featuring SiO_2 particles that are more angular and integrated, as well as higher porosity. This structure may facilitate the adsorption of organic pollutants in water through pi bonding, hydrogen bonding, and ligand binding (Li et al. 2023). Photographs of sawdust biochar at 500°C (c) show a less porous appearance with partly crushed particles, while hardwood biochar at 600°C (d) appears heterogeneous with broken fragments and a rough surface. Its microporous nature, due to a larger specific surface area and rough pore structure, makes it suitable for soil amendment and microbial carrier applications (Bolan et al. 2023).

The mass percentages of each element (C, O, Si, Ca, K, and Cl) are presented in Fig. 4 and Table 3. FMB, SDB, RHB, and HWB contain 6.87%, 80.97%, 59.85%, and 60.19% carbon, respectively. The elemental composition of finger millet biochar, as shown in Fig. 5, indicates a relatively low carbon content (61%) compared to other biochars, which typically have around 87%. The percentages of oxygen, silicon, chlorine, and potassium are 30.51%, 2.08%, 0.74%, and 4.80%, respectively. Rice husk biochar has a lower potassium content (approximately 1%) relative to FMB, along with higher silica content (8.21%) and similar carbon (59.85%) and oxygen (30.53%) levels. Sawdust biochar exhibits small quantities of oxygen (30.51%), silicon (16.57%), calcium (30.53%), and potassium (32.03%). Notably, oxygen (32.03%) and calcium (7.78%) contents are higher, while carbon (60.19%) is greater in H BW compared to others. The results also show that SDB contains less oxygen and more carbon. Potassium is only present in FMB, and calcium is found exclusively in SDB and HWB.

Table 3: Elemental analysis of biochar samples.

Biochar types	Elements [Mass %]					
	C	O	Si	Ca	K	Cl
Finger millet	61.87	30.51	2.08	-	4.80	0.74
Saw dust	80.97	16.57	0.60	1.86	-	-
Rice husk	59.85	30.53	8.21	-	1.41	-
Hardwood	60.19	32.03	-	7.78	-	-

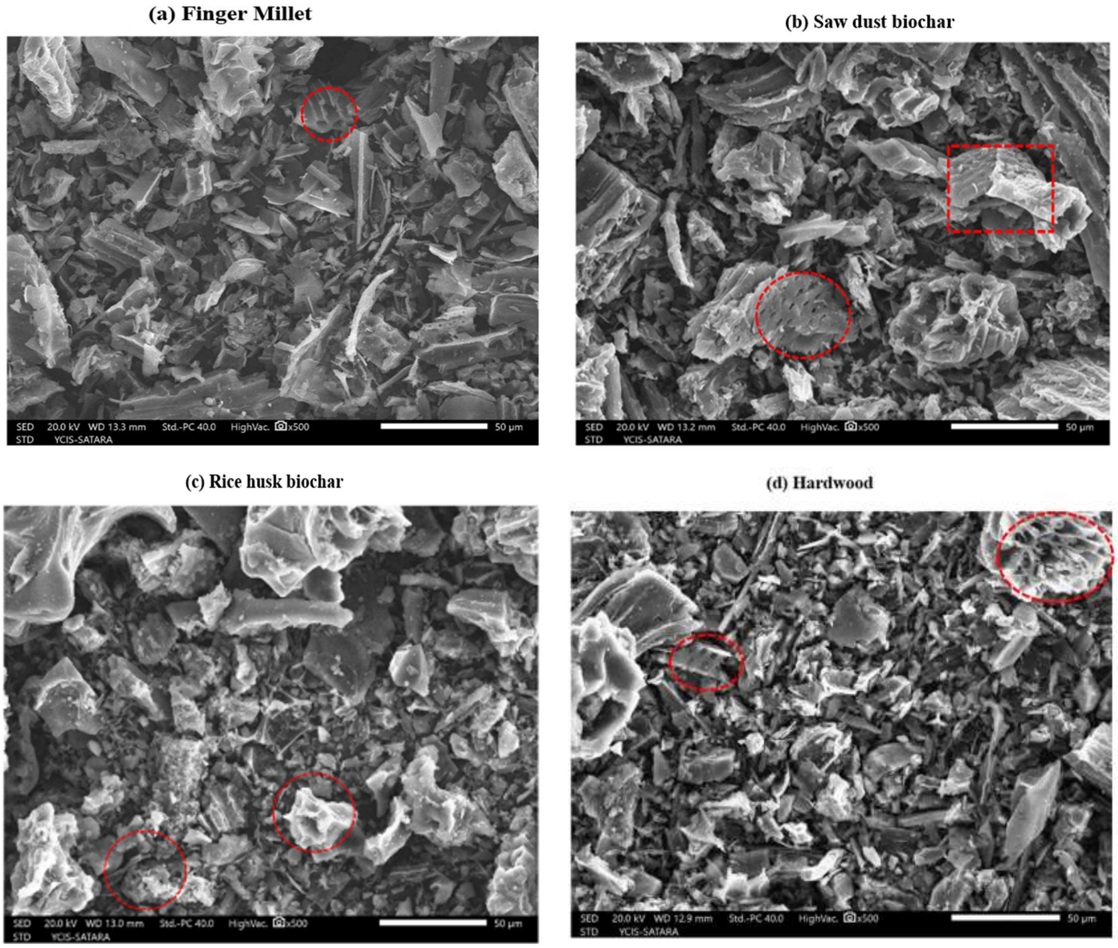

Fig. 4: SEM images of a) finger millet biochar, b) rice husk biochar, c) saw dust biochar, and d) hardwood biochar produced at 300, 400, 500 and 600°C, respectively.

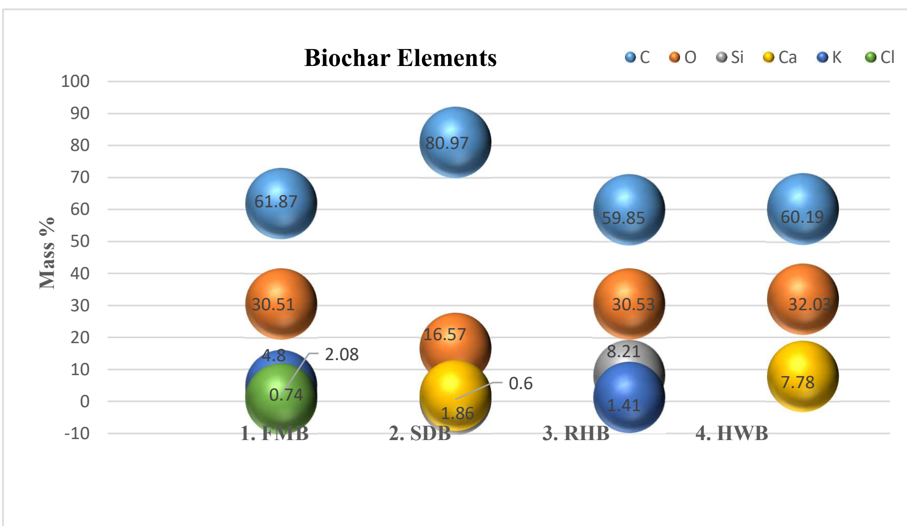

Fig. 5: Elemental composition: C, O, Si, Ca, K, Cl (%) of FMB, SDB, RHB and HWB.

4. DISCUSSION

The current study assessed how pyrolysis temperature influences the physicochemical properties, yield, elemental makeup, and surface features of biochar derived from four types of agricultural residues: sawdust, hardwood, rice husk, and finger millet hulls. As demonstrated consistently in numerous studies, pyrolysis temperature is a key factor that determines biochar quality (Mukherjee et al. 2022, Ippolito et al. 2020). Increasing the pyrolysis temperature from 300 to 600°C enhanced carbon stability, ash content, surface area, pH, and aromaticity, while it reduced biochar yield and volatile matter across all feedstocks. These findings align with the previously reported thermal decomposition behavior of lignocellulosic biomass by Qin et al. (2020) and Roshan et al. (2023).

Finger millet hull biochar (FMB), a relatively novel and underexplored precursor, exhibits characteristic flaky and fractured microstructures along with increased porosity at lower pyrolysis temperatures (300°C). These features enhance sorption capacity and support microbial colonization, aligning with findings by Zhang et al. (2021) and Varkolu et al. (2025), which indicate that adsorption and biological interactions are influenced by macroporous morphology and surface functional groups such as –OH, –COOH, and –C=O. Additionally, FMB maintains a diverse range of functional groups at lower pyrolysis temperatures, highlighting its potential for biological and environmental applications.

Hardwood biochar (HWB), produced at 600°C, exhibited the highest carbon stability, the greatest organic carbon content, increased aromaticity, and a reduction in polar surface groups. These characteristics are associated with enhanced resistance to microbial mineralization and suggest potential for long-term carbon sequestration (Bo et al. 2023, Song et al. 2023). SEM images supported previous research by Tomczyk et al. (2020) and Feng et al. (2020), confirming significant pore development and microstructural rearrangements at elevated temperatures.

In line with Li et al. (2023), rice husk biochar (RHB) showed a distinctive grainy texture and improved sorption capabilities for pollutant removal due to its higher silica content. Additionally, at 400–500°C, sawdust biochar (SDB) demonstrated a relatively high specific surface area and porosity, indicating its suitability for applications in soil improvement and water purification (Chellappan & Nair 2018).

The notion that thermal degradation concentrates mineral constituents is supported by evidence showing that nutrient levels, such as NPK, Ca, and Mg, generally increase with temperature (Khater et al. 2024). Consistent with Liu et al. (2025) and El-Naggar et al. (2019), biochars produced at higher temperatures exhibit stronger soil-enhancing effects, particularly in raising pH and enriching organic carbon. Conversely, biochars produced at lower temperatures retain more labile organic compounds, which are beneficial for stimulating soil microbial activity (Hossain et al. 2020, Akumuntu et al. 2024). This study illustrates that each biochar type offers distinct functional advantages based on feedstock composition and pyrolysis temperature. Notably, finger millet hull biochar emerges as an economically and environmentally promising option for adsorption, soil improvement, and microbial support. These results underscore biochar's versatility and call for further research on mixed feedstocks, application-specific customization, and field-scale assessments.

5. CONCLUSIONS

The effects of different thermochemical conversion temperatures (300, 400, 500, and 600°C) were examined on various agricultural residues, including finger millet hull, rice husk, sawdust, and hardwood. Converting these waste residues into biochar offers a cost-effective waste management solution, serves as a soil amendment, and contributes to environmental conservation. It was observed that the biochar's microstructure, physicochemical properties, and elemental composition were significantly affected by pyrolysis temperature. Various factors, such as biomass type, pyrolysis temperature, residence time, and heating rate, can influence biochar yield and composition. Among these, pyrolysis temperature notably affects biochar pH, yield, ash, carbon content, surface area, and porosity, while decreasing volatile matter. Lower pyrolysis temperatures tend to reduce the water-holding capacity (WHC) of biochar by producing more volatile compounds, resulting in less porous structures. The newly developed cracked finger millet hull biochar (FMB) produced at 300°C is chemically active, with a fragmented, layered surface structure and macroporosity that enhance its adsorptive capacity and potential for microbial colonization. FMB has a surface area of 28.01 $m^2.g^{-1}$ and porosity of 9.74%, making it suitable for various environmental and agricultural applications. Its surface functional groups include O-H stretches, aliphatic –CH3 and -CH2 groups, C═C-C aromatic ring stretches, trimethyl groups, and simple fluoro compounds, indicating its chemical activity in environmental contexts. As an organic macromolecule, it holds potential for use in water conservation, promoting plant growth, and improving crop yields. Additionally, treasure humic acid fertilizer contains C, O, Si, K, and Cl, with contents of 61.87%, 30.51%, 4.80%, 2.08%, and 0.74%, respectively, which can dissolve into the soil, activating beneficial microbes and enhancing crop productivity. Further research on biochar produced from blended feedstocks is recommended. Additional studies should evaluate its practicality and potential in soil improvement, environmental remediation, and climate management, in comparison to traditional fertilizers.

6. ACKNOWLEDGEMENTS

This research was financially supported by the Krishna Vishwa Vidyapeeth (Deemed to be University), Karad, Maharashtra, India.

7. REFERENCES

Abrishamkesh, S., Gorji, M., Asadi, H., Bagheri-Marandi, G. H. and Pourbabaee, A. A., 2015. Effects of rice husk biochar application on the properties of alkaline soil and lentil growth. *Plant, Soil and Environment*, 61(11), pp.1-8.

Ahmadi, S. H., Ghasemi, H. and Sepaskhah, A. R., 2020. Rice husk biochar influences runoff features, soil loss, and hydrological behavior of a loamy soil in a series of successive simulated rainfall events. *Catena*, 192, p.104587.

Ahmed, S. F., Mehejabin, F., Chowdhury, A. A., Almomani, F., Khan, N. A., Badruddin, I. A. and Kamangar, S., 2024. Biochar produced from waste-based feedstocks: Mechanisms, affecting factors, economy, utilization, challenges, and prospects. *GCB Bioenergy*, 16(8), p.e13175.

Akumuntu, A., Hong, J. K., Jho, E. H., Omidoyin, K. C., Park, S. J., Zhang, Q. and Zhao, X., 2024. Biochar derived from rice husk: Impact on soil enzyme and microbial dynamics, lettuce growth, and toxicity. *Chemosphere*, 349, p.140868.

Amalina, F., Abd Razak, A. S., Krishnan, S., Sulaiman, H., Zularisam, A. W. and Nasrullah, M., 2022. Biochar production techniques utilizing biomass waste-derived materials and environmental applications–A review. *Journal of Hazardous Materials Advances*, 7, p.100134.

AOAC, 2003. *Official Methods of Analysis of the Association of Official Analytical Chemists International*. 17th ed. Gaithersburg, MD: AOAC International, pp.1-20.

Awasthi, M. K., Duan, Y., Awasthi, S. K., Liu, T. and Zhang, Z., 2020. Influence of bamboo biochar on mitigating greenhouse gas emissions and nitrogen loss during poultry manure composting. *Bioresource Technology*, 303, p.122952.

Bo, X., Zhang, Z., Wang, J., Guo, S., Li, Z., Lin, H. and Zou, J., 2023. Benefits and limitations of biochar for climate-smart agriculture: A review and case study from China. *Biochar*, 5(1), p.77.

Bolan, S., Hou, D., Wang, L., Hale, L., Egamberdieva, D., Tammeorg, P. and Bolan, N., 2023. The potential of biochar as a microbial carrier for agricultural and environmental applications. *Science of the Total Environment*, 886, p.163968.

Chatterjee, R., Sajjadi, B., Chen, W. Y., Mattern, D. L., Hammer, N., Raman, V. and Dorris, A., 2020. Effect of pyrolysis temperature on physicochemical properties and acoustic-based amination of biochar for efficient CO_2 adsorption. *Frontiers in Energy Research*, 8, pp.1-15.

Chellappan, S. and Nair, V., 2018. Synthesis, optimization and characterization of biochar based catalyst from sawdust for simultaneous esterification and transesterification. *Chinese Journal of Chemical Engineering*, 26(12), pp.2654-2663.

Cheng, S., Liu, Y., Xing, B., Qin, X., Zhang, C. and Xia, H., 2021. Lead and cadmium clean removal from wastewater by sustainable biochar derived from poplar sawdust. *Journal of Cleaner Production*, *314*, p.128074.

Coates, J., 2000. Interpretation of infrared spectra, a practical approach. *Encyclopedia of Analytical Chemistry*, *12*, pp.10815-10837.

Dhar, S. A., Sakib, T. U. and Hilary, L. N., 2020. Effects of pyrolysis temperature on production and physicochemical characterization of biochar derived from coconut fiber biomass through slow pyrolysis process. *Biomass Conversion and Biorefinery*, 12(7), pp.2631-2647.

El-Naggar, A., Lee, S. S., Rinklebe, J., et al. 2019. Biochar application to low fertility soils: A review of current status and future prospects. *Geoderma*, 337, pp.536-554.

Feng, D., Zhang, Y., Zhao, Y., Sun, S., Wu, J. and Tan, H., 2020. Mechanism of in-situ dynamic catalysis and selective deactivation of H_2O-activated biochar for biomass tar reforming. *Fuel*, 279, p.118450.

Ge, X., Cao, Y., Zhou, B., Wang, X., Yang, Z. and Li, M. H., 2019. Biochar addition increases subsurface soil microbial biomass but has limited effects on soil CO_2 emissions in subtropical moso bamboo plantations. *Applied Soil Ecology*, 142, pp.155-165.

Gupta, S., 2019. Agriculture crop residue burning and its consequences on respiration health of school-going children. *Global Pediatric Health*, 6, p.2333794X19874679.

He, D., Luo, Y. and Zhu, B., 2024. Feedstock and pyrolysis temperature influence biochar properties and its interactions with soil substances: Insights from a DFT calculation. *Science of the Total Environment*, 922, p.171259.

Hossain, M. Z., Bahar, M. M., Sarkar, B., Donne, S. W., Ok, Y. S., Palansooriya, K. N. and Bolan, N., 2020. Biochar and its importance on nutrient dynamics in soil and plants. *Biochar*, 2(4), pp.379-420.

Ippolito, J. A., Cui, L., Kammann, C., Wrage-Mönnig, N., Estavillo, J. M., Fuertes-Mendizabal, T. and Borchard, N., 2020. Feedstock choice, pyrolysis temperature and type influence biochar characteristics: A comprehensive meta-data analysis review. *Biochar*, 2(4), pp.421-438.

Jena, P. K., Samal, S., Samal, R. R., Panigrahi, S. R., Baral, U., Behera, S., and Mishra, C. S. K., 2025. Evaluating millet biochar as mitigator of pesticide toxicity in soil using biomarkers. *iScience*, 28(4), pp.1-15.

Khater, E.S., Bahnasawy, A., Hamouda, R., Sabahy, A., Abbas, W. and Morsy, O.M., 2024. Biochar production under different pyrolysis temperatures with different types of agricultural wastes. *Scientific Reports*, 14, p.2625. [DOI]

Lan, R., Eastham, S. D., Liu, T., Norford, L. K. and Barrett, S. R., 2022. Air quality impacts of crop residue burning in India and mitigation alternatives. *Nature Communications*, 13(1), p.6537.

Li, S. and Tasnady, D., 2023. Biochar for soil carbon sequestration: Current knowledge, mechanisms, and future perspectives. *C*, 9(3), p.67. [DOI]

Li, Z., Zheng, Z., Li, H., Xu, D., Li, X., Xiang, L. and Tu, S., 2023. Review on rice husk biochar as an adsorbent for soil and water remediation. *Plants*, 12(7), p.1524. [DOI]

Liu, S., Cen, B., Yu, Z., Qiu, R., Gao, T. and Long, X., 2025. The key role of biochar in amending acidic soil: Reducing soil acidity and improving soil acid buffering capacity. *Biochar*, 7(1), p.52.

Manyuchi, M. M., Sukdeo, N. and Stinner, W., 2022. Potential to remove heavy metals and cyanide from gold mining wastewater using biochar. *Physics and Chemistry of the Earth, Parts A/B/C*, 126, p.103110.

Mathur, R. and Srivastava, V. K., 2019. Crop residue burning: Effects on environment. In: *Greenhouse Gas Emissions: Challenges, Technologies and Solutions*. Singapore: Springer Singapore, pp.127-140.

Mujtaba, G., Hayat, R., Hussain, Q. and Ahmed, M., 2021. Physico-chemical characterization of biochar, compost, and co-composted biochar derived from green waste. *Sustainability*, 13(9), p.4628.

Mukherjee, A., Patra, B. R., Podder, J. and Dalai, A. K., 2022. Synthesis of biochar from lignocellulosic biomass for diverse industrial applications and energy harvesting: Effects of pyrolysis conditions on the physicochemical properties of biochar. *Frontiers in Materials*, 9, p.870184.

Muzyka, R., Sobek, S., Dudziak, M., Ouadi, M. and Sajdak, M., 2023. A comparative analysis of waste biomass pyrolysis in Py-GC-MS and fixed-bed reactors. *Energies*, 16(8), p.3528.

Nadarajah, K., Asharp, T. and Jeganathan, Y., 2024. Biochar from waste biomass, its fundamentals, engineering aspects, and potential applications: An overview. *Water Science & Technology*, 89(5), pp.1211-1239.

Nagar, J. and Kumar, R., 2024. Agricultural residue management in India: Unlocking economic potential. *Journal of Agricultural Economics and Rural Development*, 12(3), pp.45-60.

Nandiyanto, A. B. D., Oktiani, R. and Ragadhita, R., 2019. How to read and interpret FTIR spectroscope of organic material. *Indonesian Journal of Science and Technology*, 4(1), pp.97-118.

Qin, L., Wu, Y., Hou, Z. and Jiang, E., 2020. Influence of biomass components, temperature and pressure on the pyrolysis behavior and biochar properties of pine nut shells. *Bioresource Technology*, 313, p.123682.

Rabbani, G., Hossain, M. F. and Parveen, Z., 2020. Morphological properties and nutrient status of different waste derived slow pyrolyzed biochars. *World Journal of Agriculture and Soil Science*, 6(1), pp.1-8.

Roshan, A., Ghosh, D. and Maiti, S. K., 2023. How temperature affect biochar properties for application in coal mine spoils? A meta-analysis. *Carbon Research*, 2, p.3. [DOI]

Sathyabama, K. and Firdous, S., 2025. Effect of pyrolysis temperature on the physicochemical properties and structural characteristics of agricultural waste-derived biochar. *ACS Omega*, 10(33), pp.37013-37024.

Singh, B., Camps-Arbestain, M. and Lehmann, J. (eds.), 2017. *Biochar: A Guide to Analytical Methods*. CSIRO Publishing, pp.1-20.

Song, S., Cong, P., Wang, C., Li, P., Liu, S., He, Z., Zhou, C., Liu, Y. and Yang, Z., 2023. Properties of biochar obtained from tropical crop wastes under different pyrolysis temperatures and its application on acidic soil. *Agronomy*, 13(3), p.921. [DOI]

Soothar, M. K., Mounkaila Hamani, A. K., Kumar Sootahar, M., Sun, J., Yang, G., Bhatti, S. M. and Traore, A., 2021. Assessment of acidic biochar on the growth, physiology and nutrients uptake of maize (Zea mays L.) seedlings under salinity stress. *Sustainability*, 13(6), p.3150. [DOI]

Sovova, S., Mravcova, L., Porizka, J., Kubikova, L. and Kalina, M., 2024. The effect of biochar particle size on the leaching of organic molecules and macro- and microelements. *Agronomy*, 14(10), p.2346. [DOI]

Toczydlowski, A. J., Slesak, R. A., Venterea, R. T. and Spokas, K. A., 2023. Pyrolysis temperature has greater effect on carbon and nitrogen biogeochemistry than biochar feedstock when applied to a sandy forest soil. *Forest Ecology and Management*, 534, p.120881.

Tomczyk, A., Sokołowska, Z. and Boguta, P., 2020. Biochar physicochemical properties: pyrolysis temperature and feedstock kind effects. *Reviews in Environmental Science and Bio/Technology*, *19*(1), pp.191-215.

Ulusal, A., Apaydın Varol, E., Bruckman, V. J. and Uzun, B. B., 2021. Opportunity for sustainable biomass valorization to produce biochar for improving soil characteristics. *Biomass Conversion and Biorefinery*, 11(3), pp.1041-1051.

Varkolu, M., Gundekari, S., Omvesh, Palla, V. C. S., Kumar, P., Bhattacharjee, S. and Vinodkumar, T., 2025. Recent advances in biochar production, characterization, and environmental applications. *Catalysts*, 15(3), p.243. [DOI]

Walkley, A. and Black, I. A., 1934. An examination of the Degtjareff method for determining soil organic matter, and a proposed modification of the chromic acid titration method. *Soil Science*, 37(1), pp.29-38.

Wang, P., Peng, H., Adhikari, S., Higgins, B., Roy, P., Dai, W. and Shi, X., 2020. Enhancement of biogas production from wastewater sludge via anaerobic digestion assisted with biochar amendment. *Bioresource Technology*, 309, p.123368.

Wyatalska, K., Kwarciak-Kozłowska, A. and Włodarczyk, R., 2023. Influence of technical parameters of the pyrolysis process on the surface area, porosity, and hydrophobicity of biochar from sunflower husk pellets. *Sustainability*, 15(1), p.394. [DOI]

Zhang, C., Zhang, L., Gao, J., Zhang, S., Liu, Q., Duan, P. and Hu, X., 2020. Evolution of the functional groups/structures of biochar and heteroatoms during the pyrolysis of seaweed. *Algal Research*, 48, p.101900.

Zhang, H., Cheng, Y., Zhong, Y., Ni, J., Wei, R. and Chen, W., 2024. Roles of biochars' properties in their water-holding capacity and bound water evaporation: Quantitative importance and controlling mechanism. *Biochar*, 6(1), p.30.

Zhang, P., Duan, W., Peng, H., Pan, B. and Xing, B., 2021. Functional biochar and its balanced design. *ACS Environmental Au*, 2(2), pp.115-127.